Relaxation Rate Distributions for Supercooled Liquids†

T. Franosch and W. Götze*

Physik−Department, Technische Universität München, 85747 Garching, Germany

Received: August 19, 1998; In Final Form: November 16, 1998

The mode-coupling theory for the evolution of glassy dynamics in simple liquids yields correlation functions that, outside the transient regime, can be written as a superposition of relaxators with a broad distribution of relaxation rates. The known asymptotic laws for the dynamics near an ideal glass transition imply corresponding laws for the rate distribution. We calculate the rate distributions for a hard-sphere liquid and compare them to the leading and next-to-leading asymptotic formulas.

I. Introduction

One of the salient features of the dynamics of glass-forming liquids is the sharp increase of the time scale τ of the α relaxation upon decreasing the temperature T or increasing the density n. This slow α process determines the transport coefficients such as the viscosity. Within Maxwell's theory for viscoelasticity or Debye's theory for dipole relaxation, the α relaxation contribution to the correlation functions of time t is modeled by a simple relaxator: $\Phi(t) = f\exp(-t/\tau)$. This is equivalent to a Lorentzian function of frequency ω for the susceptibility spectra $\chi''(\omega)/f = \omega\tau/[1+ (\omega\tau)^2]$. The latter describe the absorptive parts of the shear modulus and dielectric function in the theories of Maxwell and Debye, respectively.[1] Another important feature of glassy relaxation is the stretching of the dynamics over large windows of time or frequency. This observation is often accounted for by writing correlators as superpositions of Maxwell−Debye processes with a wide distribution of relaxation times τ_i; $\Phi(t) = f\sum_i g_i \exp(-t/\tau_i)$, $g_i > 0$, $\sum_i g_i = 1$. Stretching was described first by Kohlrausch, who modeled his dipole decay curves by the stretched exponential $\Phi_K(t) = f\exp - (t/\tau)^{\beta_K}$ $0 < \beta_K < 1$.[1] This Kohlrausch function is an example of the subclass of correlation functions that are called completely monotone. A function $\phi(t)$ is called completely monotone if $(-1)^n\partial^n\phi(t)/\partial t^n > 0$ for all $n = 0, 1, 2$ .... The relevance of this property is due to Bernstein's theorem which states that these functions can be written as limits of superpositions of exponentials as noted above.[2] The long-standing problem is the understanding of the distribution of g_i and τ_i, in particular, the explanation of their dependence on control parameters T and n.

The classical experiments on glassy relaxation deal with supercooled liquids for control parameters near the glass transition. The time scale τ for the α process is then many orders of magnitude larger than the one specifying the microscopic dynamics of the molecules. In this region of parameters, one can assume that the elementary steps of transport processes are activated jumps of the configurations of one or several particles over saddle points in an almost frozen potential landscape.[3] The sensitivity of the Boltzmann factors on T explains the strong temperature dependence of τ. The randomness of the potential landscape leads to distributions of activation energies and hence of relaxation times τ_i. Diezemann's recent work on stochastic rate equations is an example of how one can derive stretched α processes within such a picture.[4] Chamberlin's model is an attempt to characterize the moving units as clusters[5−8] and to study the anharmonic excitations of these complexes. This leads to a rather successful formula for the α process shape function.[9] But there is a characteristic temperature T_c such that for T approaching or exceeding T_c the picture of hopping events in a random potential loses its justification.[3]

Glassy dynamics for $T \geq T_c$ has been studied extensively in recent years. It was shown by neutron-scattering spectroscopy,[10] by depolarized light-scattering experiments,[11] and also by dielectric loss measurements[12] that the mixed salt 0.4 $Ca(NO_3)_2$/0.6 KNO_3 exhibits an α process for temperatures above $T_c \approx$ 370 K. The α process can be described in all three experiments by a Kohlrausch function with a temperature-independent stretching exponent β_K. A crucial discovery is that between the α peak of the susceptibility spectrum and the band of microscopic excitations there is an additional enhanced spectrum, referred to as β relaxation in the cited papers. It is not possible to describe the spectra in the GHz band as a sum of a conventional model for the α process and a white-noise background spectrum.[13] The hydrogen-bonded system glycerol exhibits glassy dynamics in the GHz band as shown by neutron- and light-scattering spectroscopy.[14] Also, in this case, it was shown explicitly for dielectric loss data that an interpretation of the spectra by only an α process is not possible.[15] For the van der Waals liquid *o*-terphenyl, the crossover temperature was estimated to $T_c \approx 290$ *K* on the basis of measuring the α process by neutron scattering.[16] Depolarized light-scattering spectroscopy for this system showed that the α peak can be described by a Kohlrausch function with a temperature-independent stretching exponent β_K, and this for temperatures increasing up to 86 K above the melting point.[17,18] Also, for *o*-terphenyl the β process was detected and characterized comprehensively for the light-scattering data[17] as well as for neutron-scattering results.[18] In this paper, we want to discuss the indicated new discoveries on glassy dynamics for $T > T_c$. Three questions arise naturally if one attempts to rationalize the cited experimental findings in the framework of a superposition of relaxators. To begin with, one would like to know why the Kohlrausch law is a reasonable description of a major part of the α process. Second, why are the g_i temperature independent and why are all the τ_i proportional to a common time scale τ?

* Corresponding author.

† Dedicated to Prof. C. A. Angell on the occasion of his 65th birthday.

10.1021/jp983412r CCC: $18.00
Published on Web 02/20/1999

Third, is it possible to write also the β process as a superposition of relaxators?

In recent years, the mode-coupling theory for the evolution of structural relaxation (MCT) has been develloped. Originally, this theory was proposed as a microscopic approach toward an understanding of the dynamics of cooled or compressed simple liquids.[19] The temperature T_c was identified as a parameter specifying a hidden singularity connected with an ideal liquid-to-glass transition. Asymptotic laws had been derived for the dynamics near this transition as can be inferred from the review article.[20] In the cited papers,[10−18] it was shown in detail that the data could be interpreted consistently within the MCT scenario. MCT had also provided answers to the three questions formulated at the end of the preceding paragraph. The Kohlrausch law is an exact limit result for large wave vectors **q** of MCT,[21] and all numerical work confirms that it is generally a reasonable description of the α process.[20] The temperature indepedence of g_i, τ_i/τ is an implication of the α relaxation scaling law.[22] Recently, it was shown that the glassy dynamics outside the transient deals with completely monotone functions and thus the combined $\alpha-\beta$ relaxation functions can be represented as a superposition of Maxwell−Debye processes.[23,24] Let us emphasize that this general mathematical result does not necessarily imply that the calculated correlators are averages of functions dealing with heterogeneously distributed dynamical processes.

In the preceding literature, MCT results have not been discussed as superpositions of relaxation processes. The purpose of this paper is therefore to translate the MCT scenario for the evolution of the α and β relaxation process to the language of relaxation rate distributions. Explicit numerical results will be shown for the hard-sphere system (HSS). In particular, it will be discussed how the various asymptotic laws are reflected by corresponding laws for the relaxation time distributions. The evolution of structural relaxation near the liquid−glass transition of the HSS has been studied extensively by photon correlation spectroscopy for hard-sphere colloidal suspensions,[25−27] Thus, the following calculations are of relevance for the description of the experimental data for this very simple glass-forming system.

II. Basic Formulas

In this section, we summarize the formulas connecting MCT results with expressions for relaxation rate distributions. A simple classical liquid consisting of N identical structureless particles of mass m with positions r_j at a particle number density n and inverse temperature $\beta = 1/T$ ($k_B = 1$) exhibits thermal excitations of density fluctuations $\rho_{\mathbf{q}} = N^{-1/2}\sum_j \exp(i\mathbf{q}\mathbf{r}_j)$ to wave vector **q**. Canonical averaging $\langle\ \rangle$ with respect to the Gibbs measure provides the statistical information available in an experiment.[28,29] In particular, in an X-ray scattering experiment, one deduces the static structure factor $S_q = \langle|\rho_{\mathbf{q}}|^2\rangle$, which is related to the direct correlation function c_q via the Ornstein−Zernike formula, $S_q = 1/(1 - nc_q)$; because of isotropy, it is a function of the wave vector modulus q only. The basic dynamical quantity within the theory of simple classical liquids is the normalized intermediate scattering function $\Phi_q(t) = \langle\rho_{\mathbf{q}}(t)^*\rho_{\mathbf{q}}\rangle/S_q$, which correlates density fluctuations at different times t. The mode-coupling equations of motion for a colloidal liquid, ignoring the hydrodynamic interactions, read[30]

$$\tau_q\partial_t\Phi_q(t) + \Phi_q(t) + \int_0^t m_q(t-t')\partial_{t'}\Phi_q(t')\,dt' = 0 \quad (1)$$

The time constants $\tau_q = m\beta S_q\nu/q^2$ determine the short time expansion for the correlators $\Phi_q(t) = 1 - t/\tau_q + \mathcal{O}(t^2)$. The friction constant ν is proportional to the solvent viscosity and merely sets an overall time scale. The mode-coupling approximation consists of expressing the memory kernel $m_q(t)$ as a functional of the density correlators

$$m_q(t) = \sum_{\mathbf{k}+\mathbf{p}=\mathbf{q}} V(\boldsymbol{q};\boldsymbol{k},\boldsymbol{p})\Phi_k(t)\Phi_p(t) \quad (2)$$

Here the conventional discretization of wave vectors in a unit volume is used. The nonnegative coefficients V are the equilibrium quantities[31]

$$V(\mathbf{q};\mathbf{k},\mathbf{p}) = nS_qS_kS_p\{\mathbf{q}\cdot[\mathbf{k}c_k + \mathbf{p}c_p]\}^2/(2q^4) \quad (3)$$

which vary smoothly with **q**, **k**, and **p**, and also with respect to T and n. Equations 1−3 determine the density correlator $\Phi_q(t)$. Let us remark that, apart from an overall time scale, the dynamics is determined only by experimentally available static input quantities. A hard-sphere repulsion provides a particularly simple example for the particle interaction, leaving as the single control parameter the packing fraction $\varphi = \pi nd^3/6$, where d denotes the diameter of the particles. A detailed discussion of the numerical solutions for this system has been carried out recently.[30] There appears a critical packing fraction φ_c, the analogue of the temperature T_c mentioned in the Introduction, which marks an ideal liquid−glass transition. For $\varphi < \varphi_c$, all correlators $\Phi_q(t)$ relax to zero for $t \to \infty$. However, for $\varphi \geq \varphi_c$ they acquire a nonzero long-time limit $\Phi_q(t \to \infty) = f_q > 0$. Edwards and Anderson pointed out in another context[32] that this is the signature of an ideal glass transition. It leads to an elastic contribution in the dynamic structure factor and is called the Edwards−Anderson parameter, nonergodicity parameter, glass form factor, or Debye−Waller factor. The distance to the critical point is measured conveniently by the reduced packing fraction $\epsilon = (\varphi - \varphi_c)/\varphi_c$ or more generally by the separation parameter σ, which is in leading order linearly related to ϵ by $\sigma = C\epsilon + \mathcal{O}(\epsilon^2)$. For $\varphi \to \varphi_c$, the correlators $\Phi_q(t)$ exhibit, for an intermediate time window, the β relaxation dynamics, which reads, in leading plus next-to-leading order,[30]

$$\Phi_q(t) - f_q^c = h_qG(t) + h_q[H(t) + K_qG(t)^2 + \sigma\bar{\bar{K}}_q] \quad (4)$$

The leading-order contribution, i.e., the first term on the right-hand side of eq 4, is of particularly simple form - - a product of a σ- and t-independent amplitude h_q, which includes all spatial correlations, and a wave-vector-independent, σ-sensitive function $G(t)$ that contains the dynamic information. This leading-order property is known as the factorization theorem.[33] The σ dependence of $G(t)$ can be described entirely by an amplitude scale c_σ and a time scale t_σ via the first scaling law, $G(t) = c_\sigma g_\pm(t/t_\sigma)$. The cases ± correspond to $\varphi >/< \varphi_c$. There appears a nontrivial exponent a that governs the increase of the time scale $t_\sigma = t_0|\sigma|^{-1/(2a)}$ for $\sigma \to 0$ with respect to some microscopic time t_0. The amplitude scale vanishes at the critical point, $c_\sigma = (|\sigma|)^{1/2}$. The scaling functions $g_\pm$ have been discussed comprehensively before,[34,35] and therefore, we shall recall only the basic properties needed below. For small rescaled times $\hat{t}$, it diverges as $g_\pm(\hat{t} \to 0) = \hat{t}^{-a}$, and for long times, one proves $g_+(\hat{t} \to \infty) =$ const for the glass side and $g_-(\hat{t} \to \infty) \propto -\hat{t}^b$ for the liquid side. Here occurs a second exponent b, called von Schweidler exponent, which is related to a via a transcendental equation. The range of validity of the first scaling law covers times t with $t_0 \ll t \ll t_\sigma'$, where the time scale $t_\sigma' \propto t_0/|\sigma|^\gamma$, $\gamma = 1/(2a) +$

$1/(2b)$ marks the expansion of this intermediate time window on approaching the critical point.

The bracket term of eq 4 comprises the first correction to the leading asymptote. In particular, one observes that the occurrence of the amplitudes K_q and $\bar{\bar{K}}_q$ leads to a violation of the factorization property. The new function $H(t)$ again satisfies a scaling law with the same divergent time scale; $H(t) = |\sigma|h_{\pm}(t/t_\sigma)$. The short-time and long-time behaviors of $h_\pm$ read $h_\pm(\hat{t} \to 0) \propto \hat{t}^{-2a}$ and $h_+(\hat{t} \to \infty) = \text{const}$, $h_-(\hat{t} \to \infty) \propto \hat{t}^{2b}$, respectively. Note that, for fixed $\hat{t}$, the leading correction is of the order $|\sigma|$, whereas the leading asymptote is of the order $(|\sigma|)^{1/2}$. Let us finally remark that all amplitude factors f_q, h_q, K_q, and $\bar{\bar{K}}_q$, the exponents a,b, and the scaling functions $g_\pm, h_\pm$ can be calculated from the coefficients $V(\mathbf{q}; \mathbf{k}, \mathbf{p})$ in eq 3.[30]

The solutions of eqs 1−3 are completely monotone,[23] and according to Bernstein's theorem,[2] they can be written as a superposition of Debye relaxation functions

$$\Phi_q(t) = \int_0^\infty \exp(-\gamma t)\rho_q(\gamma)\, \mathrm{d}\gamma \tag{5}$$

Here $\rho_q(\gamma)$ is a positive density. One can show in addition that for $\epsilon \neq 0$ there is a $\gamma_0 > 0$ so that $\rho_q(\gamma)$ is zero within the interval $0 < \gamma < \gamma_0$. The goal of this paper is the discussion of $\rho_q(\gamma)$. Let us emphasize that, within a given accuracy level for the description of $\Phi_q(t)$, one can evaluate eq 5 by Riemann sums. If the discretization points and weigths are denoted by $\gamma_i = 1/\tau_i$ and $g_{q,i} = \rho_q(\gamma_i)\,(\gamma_i - \gamma_{i-1})$, respectively, eq 5 reproduces the representation of the correlators as a sum of relaxators, which was discussed in the Introduction.

The numerical determination of $\rho_q(\gamma)$ from a given data set for $\Phi_q(t)$ is a formidable task. The Laplace transform, eq 5, smoothes a possibly rough object $\rho_q(\gamma)$ to an infinitely differentiable quantity $\Phi_q(t)$. Additional information on the relaxation time distribution is therefore essential. First of all, the short-time expansion for $\Phi_q(t)$ is reflected by sum rules:

$$\int_0^\infty \rho_q(\gamma)\, \mathrm{d}\gamma = 1 \tag{6}$$

$$\int_0^\infty \gamma\rho_q(\gamma)\mathrm{d}\gamma = \tau_q^{-1} \tag{7}$$

Let us introduce the inverse Laplace transforms $\mathscr{G}(\gamma)$ and $\mathscr{H}(\gamma)$ of the functions $G(t)$ and $H(t)$, respectively, by

$$G(t) = \int_0^\infty \exp(-\gamma t)\mathscr{G}(\gamma)\, \mathrm{d}\gamma \tag{8}$$

$$H(t) = \int_0^\infty \exp(-\gamma t)\mathscr{H}(\gamma)\, \mathrm{d}\gamma \tag{9}$$

The first scaling law, eq 4 is reflected in the relaxation rate density in an intermediate window of relaxation rates $1/t_\sigma' \ll \gamma \ll 1/t_0$ by

$$\rho_q(\gamma) = h_q\mathscr{G}(\gamma) + h_q[\mathscr{H}(\gamma) + K_q \int_0^\gamma \mathscr{G}(\gamma - \gamma')\mathscr{G}(\gamma')\, \mathrm{d}\gamma'] \tag{10}$$

Notice that the Laplace back transform of the plateau value f_q^c yields the contribution $f_q^c\delta(\gamma)$ to $\rho_q(\gamma)$. This contribution does not occur in the preceding equation since it was formulated under the restriction $0 < 1/t_\sigma' \ll \gamma$. The scaling properties of the functions G and H imply analogous properties for the rate densities, $\mathscr{G}(\gamma) = \sqrt{|\sigma|}t_\sigma\hat{g}_\pm(\gamma t_\sigma)$ and $\mathscr{H}(\gamma) = |\sigma|\hat{h}_\pm(\gamma t_\sigma)$, where $\hat{g}_\pm(\gamma)$ and $\hat{h}_\pm(\gamma)$ denote the densities to $g_\pm(\hat{t})$ and $h_\pm(\hat{t})$, respectively. From the asymptotic expansions for $g_\pm$ and $h_\pm$, one can derive the corresponding expansions for $\hat{g}_\pm$ and $\hat{h}_\pm$.[2] The short-time asymptote of the first scaling law is equivalent to the expansion of $\rho_q(\gamma)$ for the critical point

$$\rho_q(\gamma) = h_q(\gamma t_0)^a\{1/\Gamma(a) + [K_q + \kappa(a)](\gamma t_0)^a/\Gamma(2a)\}/\gamma, \quad 1/t_\sigma \ll \gamma \ll 1/t_0 \tag{11}$$

Similarly, for the liquid, the von Schweidler expansion is connected to the asymptote

$$\rho_q(\gamma) = h_q(\gamma t_\sigma')^{-b}\{-1/\Gamma(-b) + [K_q + \kappa(-b)](\gamma t_\sigma')^{-b}/\Gamma(-2b)\}/\gamma, \quad 1/t_\sigma' \ll \gamma \ll 1/t_\sigma \tag{12}$$

The numbers $\kappa(a)$ and $\kappa(-b)$ are extractable from the MCT functional.[30]

On the liquid side of the transition, the first scaling law terminates with the von Schweidler law, which also marks the onset of the second scaling law. This second scaling law, describing the second step of a two-step relaxation scenario, governs the relaxation of the time correlation function $\Phi_q(t)$ from the plateau value f_q^c down to zero.[20] In this regime, the shape of $\Phi_q(t)$ becomes asymptotically independent of the control parameters. Altering the control parameters such as T or n merely varies the time scale of the second relaxation step. The second scaling law reads

$$\Phi_q(t) = \tilde{\Phi}_q(t/t_\sigma') \tag{13}$$

where the time scale t_σ' has been mentioned before and the masterfunctions $\tilde{\Phi}_q$ are determined by the coefficients V at the critical point.[20] The density of relaxation rates equivalently exhibits the second scaling law for slow rates by

$$\rho_q(\gamma) = t_\sigma'\tilde{\rho}_q(\gamma t_\sigma') \tag{14}$$

where $\tilde{\rho}_q(\tilde{\gamma})$ represent the master relaxation rate densities corresponding to the $\tilde{\Phi}_q(\tilde{t})$. Let us remark that the fast-rate wing of eq 14 matches up to second order in powers of $(\gamma t_\sigma')^{-b}$ the slow−rate expansion of the first scaling law in next-to-leading order, eq 12.[30]

An alternative way of representing time correlation functions as a superposition of Debye relaxators is provided by the dimensionless density of relaxation times $\mathscr{P}_q(\tau)$ via

$$\Phi_q(t) = \int_0^\infty \exp(-t/\tau)\mathscr{P}_q(\tau)\, \mathrm{d}(\ln \tau) \tag{15}$$

where $\mathscr{P}_q(\tau)$ is connected to the relaxation rate density by $\mathscr{P}_q(\tau) = \rho_q(\gamma = 1/\tau)/\tau$. All formulas for $\rho_q(\gamma)$ can equivalently be expressed as those for $\mathscr{P}_q(\tau)$.

III. Results

Figure 1 exhibits numerical solutions for the density correlation functions of the hard-sphere system $\Phi_q(t)$ for two representative wave vectors. The discretization of the wave vector incorporates an equally spaced grid of 100 wave vector moduli with a step size of $0.4/d$ starting from $0.2/d$ up to a cutoff $q^* = 39.8/d$. The mode-coupling functional is evaluated in bipolar coordinates with the Percus−Yevick solution[28] for the static structure factor. Times are measured in units of $\nu d^2 m\beta/160$. Details on the numerical implementation can be found in ref 30. To be self-contained, let us recall some numbers for the hard-sphere system.[30] The critical point has been evaluated to $\varphi_c = 0.515\,912\,13$, the exponents read $a = 0.312$, $b = 0.583$, $\gamma = 2.46$, the time scale connecting transient dynamics to the first scaling law $t_0 = 0.425$, and the separation parameter is

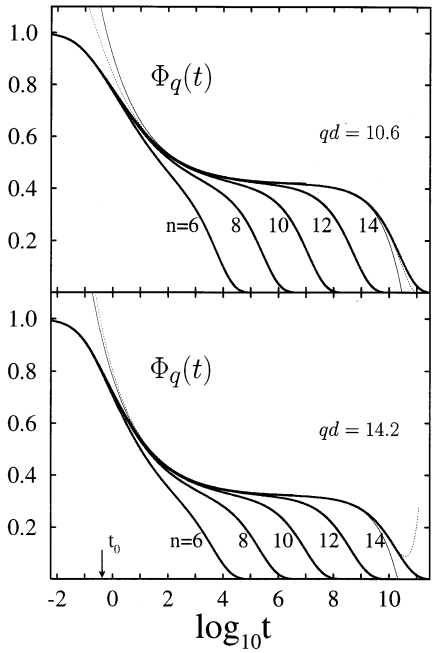

Figure 1. The correlators $\Phi_q(t)$ for a hard-sphere system as a function of time t on a logarithmic abscissa for the packing fractions $\varphi = \varphi_c(1 + \epsilon)$, $\epsilon = -10^{-n/3}$, $n = 6, 8, ..., 14$ for wave vectors $qd = 10.6$ and $qd = 14.2$. The short-time asymptote of eq 4, $\Phi_q(t) - f_q = h_q(t_0/t)^a\{1 + [K_q + \kappa(a)](t_0/t)^a\}$, in leading (light lines) and next-to-leading order (dashed lines). For $n = 14$, the long-time asymptote of eq 4, $\Phi_q(t) - f_q = -h_q(t/t_\sigma')^b\{1 - [K_q + \kappa(-b)](t/t_\sigma')^b\}$ is included in leading (light lines) and next-to-leading order (dotted lines).

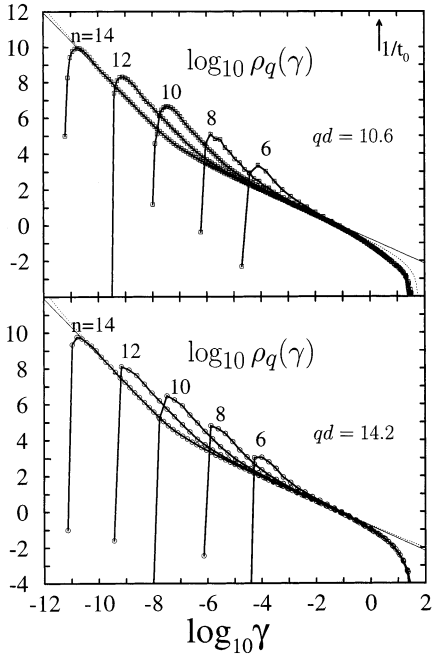

Figure 2. Rate density $\rho_q(\gamma)$ as a function of the relaxation rate γ on logarithmic scales for the results shown in Figure 1. The circles and squares indicate the discretization in the numerical inverse of the Laplace transform; the heavy lines connecting the circles and squares are guides to the eyes. The short-time and long-time asymptote of the first scaling law, eqs 11 and 12, in leading (light lines) and next-to-leading order (dotted lines) for $n = 14$.

related to the reduced packing fraction by $\sigma = C\epsilon$, $C = 1.54$. For the packing fraction closest to the critical one, the short-time and long-time asymptote of eq 4 in leading and next-to-leading order mark the range of the first scaling law. The amplitudes for wave vector $qd = 10.6$ (14.2) read $f_q^c = 0.418$ (0.321), $h_q = 0.642$ (0.599), $K_q = -0.183$ (0.070). Finally, one evaluates the numbers $\kappa(a) = -0.001$ and $\kappa(-b) = 0.569$. The transient dynamics roughly extends to times $t \approx 10$ before the correlators follow the master curve of the first scaling law. Note that for $qd = 10.6$ the leading correction enlarges the range of validity of the asymptotic description for short times by almost a decade, whereas for $qd = 14.2$, the correction amplitude $K_q + \kappa(a)$ is small and the next-to-leading order asymptote hardly differs from the leading order one. From Figure 1, one observes that the second-order term in the von Schweidler expansion increases the range of agreement of the full numerical solutions with the asymptotic expansion for both wave vectors by approximately a factor of 10. The relaxation from the plateau down to zero is the window of the second scaling law. One verifies the scaling properties by inspection; approaching the critical point merely shifts the graph for the correlators to the right on a logarithmic time scale. The shape of the master curves is different for the two wave vectors, but the time scales that describe the slowing down are coupled.[20]

To determine numerical estimates for the rate density, the integral in eq 5 was evaluated by a simple Riemann sum on a grid of logarithmically equally spaced rates between a previously chosen lowest and highest rate. The logarithmic step size was varied, and fits were obtained with step sizes from 3.3 to 11.2 rates per decade. When the squares of the weights are adjusted by a least-squares fit routine, only positive densities are considered. The error of the fit is taken as an unbiased sum of the squares of differences of the right- and left-hand sides of eq 5, including times $t \ll \tau_q$ and $t \ll t_\sigma'$. Grids are optimized to obtain a well-defined gap at slow rates and to reproduce the derived scaling laws. The results for the rate distributions for the correlators of Figure 1 are exhibited in Figure 2. The band of microscopic relaxation rates is located at the right end of the figure and hardly changes on slight increases of the density. The first scaling law dominates the distribution from somewhat above the slowest rates up to rates of the order of $1/t_0$. The increase of the relaxation rate over many decades is governed by the power laws γ^{-1+a} and γ^{-1-b}, according to the eqs 11 and 12. The q-independent master curve $\hat{g}_-$ of the first scaling law is obtained in a double logarithmic plot by a common shift of $\rho_q(\gamma)$ to the left by $\log_{10} t_\sigma$ and up by $\log_{10}(h_q(|\sigma|)^{1/2} t_\sigma)$.

For each packing fraction, there appears a slowest rate, which is manifested in the numerics by a sharp drop of the rate density over many decades. The second scaling law predicts for fixed wave vector q an asymptotic convergence to a q-dependent master curve, if on a double logarithmic plot a shift of $\rho_q(\gamma)$ is performed by the equal amount of $\log_{10} t_\sigma'$ to the left and upward. The α peak of the rate distribution, dealing with the second scaling law, appears almost structureless in this representation.

A more informative plot is provided by exhibiting the relaxation—time density according to eq 15 as shown in Figure 3 on double-logarithmic scales. Here, the band of microscopic relaxations, located at the left of the figure, is of comparable size with the peak associated to the second scaling law. In between, one observes an asymmetric minimum shifting to the lower right on approaching the critical point. The first scaling manifests itself as a smooth crossover from a decreasing τ^{-a} power law to an increasing τ^b wing. The master curve is again determined by the corresponding master curve of the rate density $\hat{g}_-$ by translating eq 2, i.e., in leading order one finds in this regime $\mathscr{R}_q(\tau) = h_q(|\sigma|)^{1/2}(t_\sigma/\tau)\hat{g}_-(\gamma t_\sigma = t_\sigma/\tau)$. The asymptotic character of this result is reflected in the observation that the range of validity of the master curve expands on approaching the critical point. This range can be quantified by evaluating

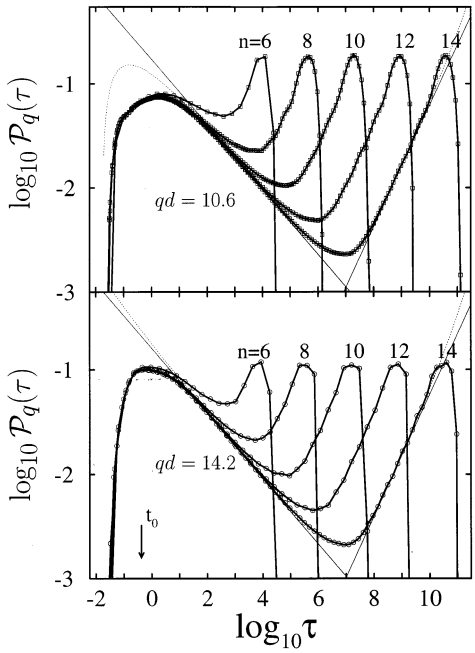

Figure 3. Rate distribution $\mathcal{P}_q(\tau)$ as a function of relaxation time τ for the results shown in Figure 1 in a double-logarithmic representation. Legend is the same as in Figure 2.

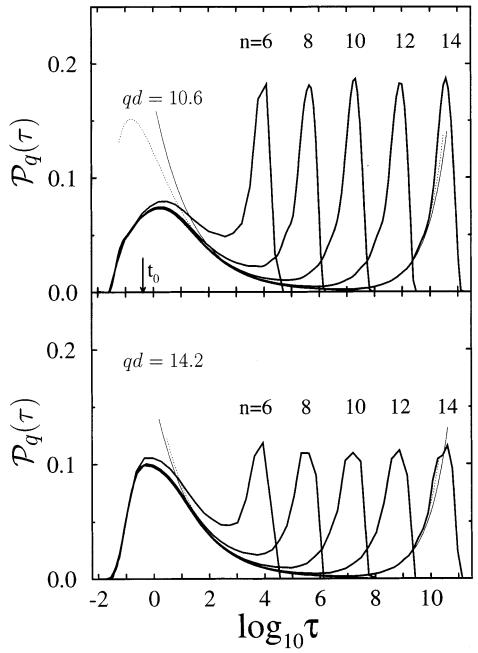

Figure 4. Rate distribution $\mathcal{P}_q(\tau)$ as a function of relaxation time τ for the results shown in Figure 1 in a semilogarithmic representation. Legend is the same as that in Figure 2.

the leading corrections to the leading order, as provided by eq 2. Two implications of the next-to-leading order results should be emphasized. First, one concludes that the deviations between the solution and the results of the first scaling law are q-dependent. Second, comparing the time correlators $\Phi_q(t)$ and the relaxation time densities $\mathcal{P}_q(\tau)$ to the corresponding master curves does not lead to the same range of validity. If t_q^* and $\tilde{t}_q^*$ mark the times where the leading correction attains a specified margin of the leading-order result on the short-time and long-time side,[30] respectively, the corresponding relaxation times τ_q^* and $\tilde{\tau}_q^*$ are connected to these number via the relation $\tau_q^* = t_q^*|\Gamma(a)/\Gamma(2a)|^{1/a}$, $\tilde{\tau}_q^* = \tilde{t}_q^*|\Gamma(-b)/\Gamma(-2b)|^{1/b}$. For the hard-sphere system, one finds $\tau_q^* = 9.20t_q^*$, $\tilde{\tau}_q^* = 0.447\tilde{t}_q^*$. Hence, on plotting the relaxation rate density instead of the time correlation functions, the range of validity of the leading-order results shrink by an overall factor of about 20. Since the minimum appears as a particularly insightful quantity, let us specialize the first scaling law to this case. Asymptotically for $\varphi \to \varphi_c$, the density of relaxation times at the minimum vanishes as $(|\sigma|)^{1/2}$, whereas the characteristic relaxation time diverges as $t_\sigma = t_0|\sigma|^{-1/(2a)}$. For example, one infers a decrease of the density at the minimum by a factor of 10 on changing $n = 3$ $\log_{10}|\epsilon|$ from 8 to 14, accompanied by a shift of the time scale to the right by approximately a factor of 1600. Let us mention that this minimum is by orders of magnitude enhanced relative to a trivial minimum, resulting from simply superposing the microscopic band and a density obtained from some Gaussian free energy barrier density. The slowest process is described by the second scaling law, which amounts on a logarithmic abscissa to a simple superposition of correlators to the same wavenumber but different densities by shifting the curves by $\log_{10}t_\sigma'$ to the left. Figure 3 demonstrates this proposition within the numerical errors.

Figure 4 exhibits the relaxation time densities from Figure 3 on a linear ordinate. The regime of the first scaling law exhibits a shallow stretched asymmetric minimum and one is tempted to ignore it all as an uninteresting background. However, there is the strong power law spectrum $1/\tau^a$ for $\tau \geq 100$ that neither can be understood as part of the α peak nor as a part of the transient. Moreover, as has been demonstrated before, the universal features of the liquid−glass transition problem are hidden just in this elusive window. The representation of Figure 4 is also not favorable for pointing at the existence of a longest relaxation time. On the other hand, Figure 4 provides the most sensitive graph for testing the predictions of the second scaling law. In particular, it demonstrates more clearly that the shape of the master curve is q-dependent. The area of the peak of the slowest process yields the Debye−Waller factor f_q^c and provides a convenient measure of the strength of the slowest structural relaxation contribution.

IV. Concluding Remarks

In this paper, we presented relaxation rate densities for a glassy hard-sphere liquid as described by the mode-coupling theory. The necessary numerical inversion of the Laplace transform is an ill-posed problem. Addition of some small noise to $\phi_q(t)$ may cause the addition of a large noise to $\rho_q(\gamma)$ via the inversion of eq 5.[36] Consider the curves shown in Figure 3 for $n = 14$. The addition of contributions to the distribution for times τ exceeding 10^{12} would not alter the correlators seriously nor would the addition of some oscillations for τ near 10^4 or 10^9. Our problem of converting MCT results for the correlators to those for rate distributions is somewhat easier than the problem one faces for the inversion of experimental results for $\phi_q(t)$. First, our input data have a noise level much smaller than the accuracy of the drawing in Figure 1, and they extend over huge time windows. Second, we know from the results (11, 12) the asymptotes shown as lines in Figure 3. Third, it is known that the distributions have a large-τ cutoff. We use this information to choose our cutoff and the spacing of the rate discretization so that conflicts with the cited results are avoided. Thus, the combination of these high-precision data with analytic formulas for the first scaling law allows for a sound approximation to the true relaxation rate density.

Approximating the continuous wave vector set by a finite set of representative wave vector moduli, i.e., replacing the continuous sum in eq 2 by Riemann approximands, introduces

new qualitative features. The discretized model exhibits a gap in the density of relaxation rates for packing fractions different from φ_c. However, for fixed $\varphi \neq \varphi_c$, hydrodynamics requires larger and larger wavelength fluctuations to relax slower and slower. For our colloid model, the rate of decay for density fluctuations vanishes as Dq^2 for $q \to 0$, where D is the diffusion coefficient. The nonzero small wave vector cutoff introduced by the discretization excludes the true limit $1/\tau_q \propto Dq^2 \to 0$. By refining the discretization grid, one can capture part of the hydrodynamic relaxation. Then, the results for intermediate wave vectors are found not to change appreciably in the time domain. In terms of rates, one expects therefore only a small tail smearing the gap in the rate distribution to a crossover.

A second consequence of wave vector discretization has its origin in ignoring contributions coming from the limit $q \to \infty$. As mentioned in the Introduction, a popular fitting function for the α process is the Kohlrausch law $\Phi_q(t) = f_q \exp -(\Gamma_q t)^{\beta_K}$, $\beta_K < 1$. Its theoretical justification stems from the theory of probability.[2] The probability distribution of the sums of many independent processes is determined by limit theorems. If and only if the variance exists, Gauss' central limit theorem yields the normal distribution, i.e., the Kohlrausch law for $\beta_K = 2$. Otherwise, according to Levy's theory, a limit distribution follows whose characteristic function is the Kohlrausch law for $\beta_K < 2$. The request of complete monotonicity is equivalent to $\beta_K \leq 1$. The Laplace transform to frequency z, which we use with the convention $\Phi_q(z) = i\int_0^\infty \exp(izt)\Phi_q(t)\,dt$, of the completely monotone $\Phi_q(t)$ can be continued to an analytic function in the complex plane with the possible exception of the negative imaginary axis. If the origin of the complex plane also admits an analytical continuation, the corresponding series expansion in the frequency domain has a nonzero radius of convergence that is determined by the moments $\omega^{(n)} = \int_0^\infty t^n\Phi(t)\,dt$. For the Kohlrausch function, all moments turn out to be finite; however, the corresponding series does not converge for $z \neq 0$. As a consequence, there is no smallest relaxation rate $\gamma_0 > 0$ for this case. However, the Kohlrausch law is also the large-q solution for the second scaling law of the MCT equations.[21] The apparent contradiction is resolved by observing that the limits $\varphi \to \varphi_c$ and $q \to \infty$ do not commute. When the critical point is approached, the gap is filled on a characteristic rate scale for the second scaling law $\gamma \propto 1/t_\sigma'$. The convergence to Kohlrausch functions for small distances with respect to rates is not uniform on the scale of the second scaling law. The dimensionless coefficient $\Gamma_q\, t_\sigma'$ diverges proportional to $q^{1/b}$ [21], and consequently, the peak of the relaxation rate density separates to faster rates. The deviations from the Kohlrausch law are most important for rates smaller than Γ_q, explaining the difference between a true gap for $\varphi \neq \varphi_c$ within the discretized model and the exponentially small relaxation-rate density for the Kohlrausch law.

Completely monotone functions can be represented as a superpostion of deacaying exponentials; however, in general, one has to replace $\rho_q(\gamma)\,d\gamma$ in eq 5 by a positive measure $d\alpha_q(\gamma)$ derived from an increasing weight function $\alpha_q(\gamma)$. The rate densities presented in the figures suggest that this weight function $\alpha_q(\gamma)$ is absolutely continuous. Such a suggestion is misleading however. Within the prescribed error margin for $\Phi_q(t)$, one can always replace $\alpha_q(\gamma)$ by a differentiable function. Our numerical procedure cannot decide whether $\alpha_q(\gamma)$ is absolutely continuous.

However, for the wave vector discretized model one can prove that for $\varphi < \varphi_c$ the measure $\alpha_q(\gamma)$ is a step function and the set of discontinuities is free of accumulation points. A sketch of the proof follows. The existence of a gap for the correlator,[23] i.e., $\Phi_q(t) = \mathcal{O}(e^{-\gamma_0 t})$, implies by eq 2 the same property for the memory kernel $m_q(t)$, and one concludes even $m_q(t) = \mathcal{O}(e^{-2\gamma_0 t})$. In particular, this ensures that its Laplace transform $m_q(z)$ is holomorphic for $\Re z > -2\gamma_0$. The representation of eq 1 in the frequency domain

$$\Phi_q(z) = -1/\{z - 1/[i\tau_q + m_q(z)]\} \tag{16}$$

implies that $\Phi_q(z)$ is meromorphic for $\Re z > -2\gamma_0$ with at most a single simple pole above the line $\Re z = -2\gamma_0$. Since $\Phi_q(t)$ is completely monotone, the possible pole then is necessarily located on the negative imaginary axis and has a positive residue. Therefore, one can write $\Phi_q(t) = \hat{f}_q^{(0)} e^{-\gamma_q^{(0)}} + \mathcal{O}(e^{-2\gamma_0 t})$, $0 \leq \hat{f}_q^{(0)} \leq 1$, $\gamma_0 < \gamma_q^{(0)} < 2\gamma_0$. Now, one can iterate the argument. The memory kernel allows for representation as a finite sum of relaxators with positive weights and relaxation rates between γ_0 and $2\gamma_0$ and a remainder that can be estimated by $\mathcal{O}(e^{-4\gamma_0 t})$. This in turn implies that in the half space $\Re z > -4\gamma_0$ only a finite number of poles exists and $m_q(z)$ is meromorphic there. The Zwanzig−Mori representation, eq 16, then shows that the rates slower than $4\gamma_0$ are discretely distributed. Continuing the chain of arguments, one finds $\Phi_q(t)$ and $m_q(t)$ to be a sum of exponentials with at most a finite number of exponents $\gamma_i = 1/\tau_i$ to the left of $n\gamma_0$, with $n > 0$ being arbitrary. Obviously, the proof remains valid if the mode-coupling functional in eq 2 is extended by adding monomials of three or more factors of $\Phi_k(t)$. If, however, $m_q(t)$ contains also a linear mode-coupling contribution, one can show that $\alpha_q(\gamma)$ is differentiable with respect to γ except for a discrete set of γ_i without accumulation points.

The relaxational dynamics of the colloid model is essential for a representation of the complete correlators as a superposition of Debye relaxators. Newtonian dynamics does not lead to absolutely monotone correlators, as is most strikingly manifested in the existence of sound waves. However, the dynamics within the window of the first and the second scaling law is asymptotically independent of the underlying time evolution operator. The microscopic equations of motion merely enter the first and second scaling via a time scale t_0. Thus, the shape of the correlators, rate densities, or susceptibilities in the mentioned window is independent of the microscopic details for the transient if they are plotted on a logarithmic abscissa as has been discussed recently.[24] Accordingly the relaxation time densities discussed in this paper are not restricted to the hard-sphere colloid model but equally apply to the Newtonian hard-sphere liquid outside the transient dynamics.

The representation of the structural relaxation in terms of a distribution of rates suggests an interpretation of independently relaxing cooperative clusters. Each cluster is thereby characterized by a single relaxation rate connected by an Arrhenius relation to some free energy barrier. The evaluation of the relaxation rate density amounts in this picture to the determination of the cluster statistics. The log τ axis for fixed density (or temperature in simple van der Waal's liquids) is then proportional to the free energy barrier distribution. The solutions of the mode-coupling equations show that this distribution is changing rapidly on approaching the critical point. It cannot be obtained by a mere scale transformation on the abscissa since the evolution of the dynamics with changes of control parameters is governed by two critical time scales t_σ and t_σ' rather than by one scale only. In fact, the exponents a and b are not density (temperature) dependent, but the range of validity of the first scaling law extends with $\varphi \to \varphi_c$. The second scaling

law, i.e., the time density (temperature) superposition principle, is hardly reconcilable with a free energy barrier approach. One has to explain the coherent increase of activation barriers, which is in our opinion the major challenge to a theory of the glass transition. Furthermore, the distribution of free energies is not simple, as can be inferred from Figures 2−4. A log normal distribution or Poisson distribution of free energy barriers may be appropriate for fitting the shape of the α relaxation function; it does not cover, however, the anomalous dynamics in the window of the first structural relaxation law. The two-step scenario predicted by MCT explains the features found in experiments.[10−18] The contents of the MCT results can be discussed in time, frequency, and rate space as presented here. Our results do not supply any support for the idea that glassy relaxation for $T > T_c$ can be explained within a picture of a heterogeneous distribution of clusters, with each cluster exhibiting a simpler dynamics than that described by the averaged correlators.

The qualitative features of the MCT scenario for the correlators and spectra have been verified to some extend for some conventional glass-forming systems by the experiments quoted in the preceding paragraph. Since correlators or spectra are mathematically equivalent to the rate distributions, one concludes that also our results in Figures 2−4 reflect the qualitative features of the reality. It was shown[25−27] that the MCT results for the hard-sphere system account quantitatively for the correlation functions $\phi_q(t)$ measured near the glass transition of colloidal suspensions of hard spheres. Thus, one concludes that the results in Figures 2−4 are quantitative findings valid for the cited very simple glass-forming system. Our rewriting of the MCT results in form of the Figures 2−4 shows what an alternative theory for the rate distributions in glassy liquids for $T > T_c$ has to explain.

Acknowledgment. We thank H. Z. Cummins and M. Fuchs for many stimulating discussions and a critical reading of the manuscript. We are grateful to A. P. Singh and M. R. Mayr for discussions and providing us with the correlation functions $\Phi_q(t)$. Our work was supported by Verbundprojekt BMBF 03-G05TUM.

References and Notes

(1) Wong, J.; Angell, C. A. *Glass: Structure by Spectroscopy*; (Marcel Dekker: New York, 1976.

(2) Feller, W. *Introduction to Probability Theory*, 2nd ed.; Wiley: New York, 1971; Vol. II.

(3) Goldstein, M. *J. Chem. Phys.* **1969**, *51*, 3728.

(4) Diezemann, G. *J. Chem. Phys.* **1997**, *107*, 10112.

(5) Chamberlin, R. V.; Böhmer, R.; Sanchez, E.; Angell, C. A. *Phys. Rev. B* **1992**, *46*, 5787.

(6) Chamberlin, R. V. *Phys. Rev. B* **1993**, *48*, 15638.

(7) Chamberlin, R. V.; Kingsbury, D. W. *J. Non-Cryst. Solids* **1994**, *172−174*, 318.

(8) Schiener, B.; Loidl, A.; Chamberlin, R. V.; R. Böhmer, *J. Mol. Liq.* **1996**, *69*, 243.

(9) Hansen, C.; Richert, R.; Fischer, E. W. *J. Non-Cryst. Solids* **1997**, *215*, 293.

(10) Mezei, F. *Ber. Bunsen-Ges. Phys. Chem.* **1991**, *95*, 1118.

(11) Li, G.; Du, W. M.; Chen, X. K.; Cummins, H. Z.; Tao, N. J. *Phys. Rev. A* **1992**, *45*, 3867.

(12) Lunkenheimer, P.; Pimenov, A.; Loidl, A. *Phys. Rev. Lett.* **1997**, *78*, 2995.

(13) Cummins, H. Z.; Li, G.; Du, W. M.; Hernandez, J.; Tao, N. J. *Transp. Theory Stat. Phys.* **1995**, *24*, 981.

(14) Wuttke, J.; Hernandez, J.; Li, G.; Coddens, G.; Cummins, H. Z.; Fujara, F. Petry, W.; Sillescu, H. *Phys. Rev. Lett.* **1994**, *72*, 3052.

(15) Lunkenheimer, P.; Pimenov, A.; Dressel, M.; Goncharov, Yu. G.; Böhmer, R.; Loidl, A. *Phys. Rev. Lett.* **1996**, *77*, 318.

(16) Petry, W.; Bartsch, E.; Fujara, F.; Kiebel, M.; Sillescu, H.; Farago, B. *Z. Phys. B* **1991**, *83*, 175.

(17) Cummins, H. Z.; Li, G.; Du, W.; Hwang, Y. H.; Shen, G. Q. *Prog. Theor. Phys. Suppl.* **1997**, *126*, 21.

(18) Tölle, A.; Schober, H.; Wuttke, J.; Fujara, F. *Phys. Rev. E* **1997**, *56*, 809.

(19) Bengtzelius, U.; Götze, W.; Sjölander, A. *J. Phys. C* **1984**, *17*, 5915.

(20) Götze, W.; Sjögren, L. *Rep. Prog. Phys.* **1992**, *55*, 241.

(21) Fuchs, M. *J. Non-Cryst. Solids* **1994**, *172−174*, 241.

(22) Götze, W. In *Amorphous and Liquid Materials*; NATO ASI Series; Lüscher, E., Fritsch, G., Jacucci, G., Eds.; Martinus Nijhoff Publishers: Dordrecht, 1987; p 34.

(23) Götze, W.; Sjögren, L. *J. Math. Analysis Appl.* **1995**, *195*, 230.

(24) Franosch, T.; Götze, W.; Mayr, M. R.; Singh, A. P. *J. Non-Cryst. Solids* **1998**, *235−237*, 71.

(25) van Megen, W.; Underwood, S. M. *Phys. Rev. Lett.* **1993**, *70*, 2766.

(26) van Megen, W.; Underwood, S. M. *Phys. Rev. E* **1993**, *47*, 248.

(27) van Megen, W.; Underwood, S. M. *Phys. Rev. E* **1994**, *49*, 4206.

(28) Hansen, J.-P.; McDonald, I. R. *Theory of Simple Liquids*, 2nd ed.; Academic Press: London, 1986.

(29) Balucani, U.; Zoppi, M. *Dynamics of the Liquid State*; Clarendon Press: Oxford, 1994.

(30) Franosch, T.; Fuchs, M.; Götze, W.; Mayr, M. R.; Singh, A. P. *Phys. Rev. E* **1997**, *55*, 7153.

(31) Sjögren, L. *Phys. Rev. A* **1980**, *22*, 2866.

(32) Edwards S. F.; Anderson, P. W. *J. Phys. F* **1975**, *5*, 965.

(33) Götze, W. *Z. Phys. B* **1985**, *60*, 195.

(34) Götze, W. *J. Phys.: Condens. Matter* **1990**, *2*, 8485.

(35) Götze, W. In *Liquids, Freezing and Glass Transition*; Hansen, J.-P., Levesque, D., Zinn-Justin J. Eds.; North-Holland: Amsterdam, 1991; p 287.

(36) Davis, P. J.; Rabinowitz, P. *Methods of numerical integration*; Acad. Press: New York, 1975.